Campbell Response in Type-II Superconductors under Strong Pinning Conditions

R. Willa,[1] V. B. Geshkenbein,[1] R. Prozorov,[2] and G. Blatter[1]

[1]*Institute for Theoretical Physics, ETH Zurich, 8093 Zurich, Switzerland*
[2]*The Ames Laboratory and Department of Physics and Astronomy, Iowa State University, Ames, Iowa 50011, USA*

Measuring the ac magnetic response of a type II superconductor provides valuable information on the pinning landscape (pinscape) of the material. We use strong pinning theory to derive a microscopic expression for the Campbell length λ_C, the penetration depth of the ac signal. We show that λ_C is determined by the jump in the pinning force, in contrast to the critical current j_c, which involves the jump in pinning energy. We demonstrate that the Campbell lengths generically differ for zero-field-cooled and field-cooled samples and predict that hysteretic behavior can appear in the latter situation. We compare our findings with new experimental data and show the potential of this technique in providing information on the material's pinscape.

Technologically useful superconductors are of second type and acquire their desired transport and magnetic properties through vortex pinning; i.e., vortices [1] get immobilized by material defects. Understanding and characterizing the underlying pinning landscape (or pinscape) is of great importance but presents quite a formidable task, with implications reaching beyond superconductivity, e.g., in studies of disordered polymers [2] or magnetic domain walls [3]. Measurements of dc transport properties, either dynamically through the current–voltage characteristic [4] or statically through magnetization [5], are standard techniques to gain information on the pinscape. Similarly, the ac magnetic response of superconducting samples [6] provides insight into the shape of pinning potentials. Unfortunately, the relation between the measured penetration depth of the ac signal, the so-called Campbell length λ_C, and the parameters of the pinscape is only known on a phenomenological level. In this Letter, we present a microscopic derivation of the Campbell length within the framework of strong pinning theory, thereby providing access to microscopic parameters of pinning defects and substantially enlarging the scope of applications of this measurement technique.

Probing superconductors via their ac magnetic response goes back to the 1960s and culminated in Campbell's work [6], which provided the first consistent explanation of the penetration phenomenon (see Ref. [7] for further developments): for small ac magnetic-field amplitudes h_{ac} and frequencies ω, vortices oscillate reversibly within their pinning potentials (described as harmonic wells $\alpha x^2/2$), with the external signal h_{ac} penetrating the sample on a distance $\lambda_C \propto B/\sqrt{\alpha}$ of order micrometers. Later work by Lowell [8] and Campbell [9] provided a more quantitative but still phenomenological understanding within a model pinscape. Here, we make use of the strong pinning scenario allowing us to perform a quantitative and microscopic analysis of the ac magnetic response. In particular, we find the dependence of the Campbell penetration depth λ_C on the vortex state, e.g., the Bean critical [or zero-field-cooled

(ZFC)] state [5] state with a vortex density gradient supporting the critical current density j_c [10] or a field-cooled (FC) state with a constant induction B, and predict the occurrence of new hysteretic effects. The comparison with recent experiments [11] confirms our predictions.

Consider a superconductor occupying the half-space $X > 0$, the magnetic induction $B(X, t) = B_0 + \delta B(X, t)$ directed along Z, and the screening current j flowing along Y (capital and lower case letters distinguish between macroscopic and microscopic coordinates). The equation of motion for the macroscopic vortex displacement $U(X, t)$ reads

$$\eta \partial_t U = F_L(j, U) + F_{pin}(X, U), \qquad (1)$$

with the Lorentz force F_L balanced by dissipative and pinning forces (η denotes the viscosity [12]). The displacement $U(X, t)$ relates to the induction via $\delta B(X, t) = -B_0 \partial_X U(X, t)$ and is driven at the surface $X = 0$ by the small external field $h_{ac} \ll B_0$, $\delta B(0, t) = h_{ac} e^{-i\omega t}$. The Lorentz force $F_L = (j_0 + \delta j)B/c$ involves an ac component $\delta j = -c \partial_X \delta B/4\pi$, and writing the pinning force $F_{pin} = F_0 + \delta F_{pin}$, with F_0 the force density in the initial vortex state balancing the dc Lorentz force $j_0 B_0/c$, we obtain the dynamical equation

$$\eta \partial_t U - (B_0^2/4\pi)\partial_X^2 U - \delta F_{pin}(U) = 0. \qquad (2)$$

Following Ref. [6], one assumes small oscillations of the vortices near the potential minima. This motivates the phenomenological ansatz $\delta F_{pin}(U) = -\alpha U$ for the pinning force density. Solving Eq. (2) for the displacement field,

$$U(X, t) = \lambda_C(h_{ac}/B_0)e^{-X/\lambda_C}e^{-i\omega t}, \qquad (3)$$

$$\text{with} \quad \lambda_C^2(\omega) = B_0^2/4\pi(\alpha - i\omega\eta), \qquad (4)$$

results in the Campbell length $\lambda_C = \lambda_C(\omega = 0) = (B_0^2/4\pi\alpha)^{1/2}$ at low frequencies.

Here, our goal is to derive an expression for δF_{pin} starting from a microscopic perspective. This can be done within the framework of strong pinning theory, which goes back to the works of Labusch [13] and Larkin and Ovchinnikov [14], with recent further studies on the critical currents in strong and weak pinning scenarios [15], numerical simulations of vortex motion [16], and the current–voltage characteristic [17]; note that the qualitative framework of weak collective pinning theory [14] is not sufficient to develop a quantitative understanding of λ_C.

Consider a representative vortex within the flux lattice driven along x on a trajectory described through the asymptotic coordinate $\mathbf{r}_\infty = (x, b)$ at large $|z|$; the distance b along y is the impact parameter with respect to a defect at the origin. Within the strong pinning context, defects act individually, generating a pinning potential $e_p(r, z)$. Considering a trajectory with maximal pinning, i.e., $b = 0$ and including the deformation energy of the vortex, its total energy as a function of x takes the form (we assume a pointlike defect with $e_p(x, z) = e_p(x)\delta(z)$, see Ref. [15])

$$e_{\mathrm{pin}}(x) = \frac{1}{2}\bar{C}u(x)^2 + e_p[x + u(x)], \quad (5)$$

with $u(x)$ the microscopic displacement field in the plane $z = 0$, see Fig. 1, and $\bar{C}$ the effective elasticity of the vortex embedded within the lattice,

$$\bar{C}^{-1} = \frac{1}{2}\int \frac{d^3k}{(2\pi)^3}\frac{1}{c_{66}(k_x^2 + k_y^2) + c_{44}(\mathbf{k})k_z^2}. \quad (6)$$

Here, c_{66} and $c_{44}(\mathbf{k})$ denote shear and dispersive tilt moduli and proper integration in Eq. (6) provides the result $\bar{C} \sim (a_0^2/\lambda)\sqrt{c_{66}c_{44}(0)}$, with $a_0^{-2} = B_0/\Phi_0$ the vortex density ($\Phi_0 = hc/2e$ is the flux unit and λ the London penetration depth). Minimization of Eq. (5) with respect to u (at fixed x) generates the self-consistency condition,

$$\bar{C}u(x) = f_p[x + u(x)], \quad (7)$$

for the displacement field $u(x)$, where $f_p(x) = -e_p'(x)$ is the bare force profile of the pinning defect, the prime denoting derivative with respect to x. The maximal slope in $f_p(x)$, realized at x_m, defines the regime of strong pinning [13]: for $\kappa \equiv [f_p'(x_m)]/\bar{C} > 1$, the condition in Eq. (7) generates two stable solutions for the displacement field $u(x)$, a pinned and an unpinned branch; see Fig. 1. The condition $\kappa = 1$ is the famous Labusch criterion [13] separating strong ($\kappa > 1$) from weak ($\kappa < 1$) pins.

Assuming a homogeneous random distribution of defects with small density n_p (see below for a quantitative criterion), the macroscopic pinning force density F_{pin} derives from averaging the pinning forces $f_p[x + u_o(x)]$ over all positions $|x| < a_0/2$ within a lattice period, with u_o denoting the branch occupied with vortices. This
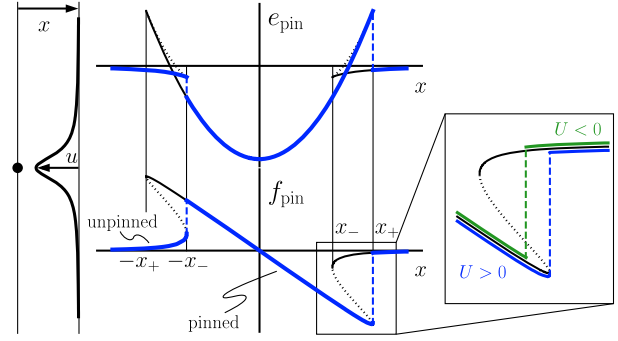

FIG. 1 (color online). Pinning energy e_{pin} and force f_{pin} in a strong pinning situation for a Lorentzian potential. The bistable solutions near the defect describe pinned and unpinned branches. Thick lines (blue) mark occupied branches in the Bean state, dotted lines are unstable solutions, dashed lines are the jumps making up for Δe_{pin} and Δf_{pin}. Left: Strong pinning situation for a representative vortex. The microscopic displacement $u(x) = f_{\mathrm{pin}}(x)/\bar{C}$ has the same shape as $f_{\mathrm{pin}}(x)$. Right: Change in branch occupation when the vortex system moves by U.

occupation depends on the state preparation, e.g., for a Bean state with vortices driven along x, the occupation of the pinned branch extends over the interval $[-x_-, x_+]$, see Fig. 1, such as to produce the maximal force $F_{\mathrm{pin}} = -F_c$,

$$F_c = -n_p\langle f_{\mathrm{pin}}\rangle = -n_p\frac{t_\perp}{a_0}\int_{a_0}\frac{dx}{a_0}f_{\mathrm{pin}}(x)|_o, \quad (8)$$

where $f_{\mathrm{pin}}(x) \equiv f_p[x + u(x)]$ and $|_o$ refers to the occupied branch $u_o(x)$ (we assume maximal pinning for all trajectories with $2|b| < t_\perp \simeq \xi$, ξ the coherence length). Making use of Eqs. (5) and (7), we derive the relation $f_{\mathrm{pin}}(x) = -de_{\mathrm{pin}}(x)/dx$ and arrive at a simple expression for the critical current density $j_c = (c/B_0)F_c$,

$$j_c = \frac{c}{B_0}n_p\frac{t_\perp}{a_0^2}\int_{a_0}dx[-de_{\mathrm{pin}}(x)/dx|_o] = \frac{cn_pt_\perp}{\Phi_0}\Delta e_{\mathrm{pin}}, \quad (9)$$

where Δe_{pin} is the sum of jumps at $-x_-$ and x_+ in $e_{\mathrm{pin}}(x)$, where the occupation changes between unoccupied and occupied branches [13,14]; see Fig. 1.

Equipped with this microscopic understanding of pinned vortex matter, we return to the problem of ac magnetic response. Within strong pinning, we can follow the changes in the occupation of pinned and unpinned branches as vortices are driven by the ac-magnetic field and determine the time-dependent and inhomogeneous change in the pinning force $\delta F_{\mathrm{pin}}[U(X, t)]$. A macroscopic shift $U > 0$ pushes vortices in the critical direction of the Bean state; vortices at $-x_-$ and x_+ jump to pinned and unpinned branches, respectively, leaving the (critical) branch occupation unchanged and, hence, $\delta F_{\mathrm{pin}}(U > 0) = 0$. On the other hand, for a negative displacement $U < 0$, vortices

relax back in their pinning wells and the boundaries between occupied and unoccupied states are shifted to the left; see Fig. 1. This results in a change of the macroscopic restoring force,

$$\delta F_{\text{pin}}(U<0) = n_p \frac{t_\perp}{a_0^2} \int_{a_0} dx [f_{\text{pin}}(x)|_{o,U} - f_{\text{pin}}(x)|_{o,0}], \quad (10)$$

where the index $|_{o,U}$ refers to the occupation where vortices have been shifted by U. Expanding the integrand for small U, we arrive at the expression

$$\delta F_{\text{pin}}(U<0) = n_p \frac{t_\perp}{a_0^2} \int_{a_0} dx df_{\text{pin}}(x)/dx|_o U, \quad (11)$$

resulting in the strong pinning result for δF_{pin},

$$\delta F_{\text{pin}}(U) = -n_p(t_\perp/a_0^2)\Delta f_{\text{pin}}\Theta(-U)U, \quad (12)$$

with Δf_{pin} the sum of jumps in the function f_{pin}.

Inserting this result into Eq. (2) generates a complex vortex dynamics as flux enters the sample in a sequence of diffusive pulses until the field is raised to $B_0 + h_{\text{ac}}$; see [18] for a detailed description of this initialization process. After saturating the sample at this higher field level, the displacement $U(X,t)$ assumes the form

$$U(X,t) = U_0(X) - \lambda_C(h_{\text{ac}}/B_0)e^{-X/\lambda_C}[1 - e^{-i\omega t}], \quad (13)$$

with $U_0(X) = (-h_{\text{ac}}X + \phi)/B_0$ generating the shift in field $B_0 \to B_0(1 - \partial_X U_0) = B_0 + h_{\text{ac}}$ and ϕ denoting the total flux (per unit length along Y) that has entered the sample [19]. The second term accounts for the penetration of the external field with respect to the *new* Bean state, $\delta B(X,t) = h_{\text{ac}}e^{-X/\lambda_C}(1 - e^{-i\omega t})$. The Campbell penetration depth can be expressed by the microscopic parameters, the average curvature $d^2 e_{\text{pin}}(x)/dx^2$, of the pinscape,

$$\frac{B_0^2}{4\pi\lambda_C^2} = -\frac{n_p t_\perp}{a_0^2} \int_{a_0} dx d^2 e_{\text{pin}}(x)/dx^2|_o = \frac{n_p t_\perp}{a_0^2}\Delta f_{\text{pin}}. \quad (14)$$

Making use of the estimates $\Delta f_{\text{pin}} \sim f_p$, $t_\perp \sim \xi$, and $\kappa \sim f_p/\xi\bar{C}$, we find that $\lambda_C^2 \sim \lambda^2/(\kappa n_p a_0 \xi^2) > \lambda^2$, with $\kappa n_p a_0 \xi^2 \ll 1$ the small parameter defining the three-dimensional strong pinning regime [15]. Comparing the results for j_c and λ_C^{-2} [Eqs. (9) and (14) with $\Delta e_{\text{pin}} \sim f_p^2/\bar{C}$], we observe that these two quantities address different properties of the pinscape, the jumps in pinning energy and force, respectively. As a consequence, the simple scaling $j_c \sim c\alpha\xi/B_0 \sim (c/4\pi)\xi B_0/\lambda_C^2$ previously conjectured on the basis of the phenomenological result [Eq. (4)] turns out incorrect and has to be replaced by $j_c \sim (c/4\pi)\kappa\xi B_0/\lambda_C^2 \propto [\Delta f_{\text{pin}}]^2$. Hence, care must be taken when translating measured data on λ_C into predictions for j_c [11].

Next, we turn to the field-cooled state with $j_0 = 0$ and $F_0 = 0$. Following Eq. (14), the determination of the jumps in the, now symmetric, occupation of f_{pin} is the central task in the calculation of λ_C. Assuming defects in the form of metallic or insulating inclusions, one can show [20] that pinning turns on smoothly upon crossing the $H_{c2}(T)$ line. Hence, the vortex system changes from weak to strong pinning upon decreasing the temperature T below the Labusch temperature T_L defined through $\kappa(T_L) = f_p'(x_m)/\bar{C}|_{T_L} = 1$. At T_L, the pinning force $f_{\text{pin}}(x)$ for the first time develops an infinite slope at x_{0L}, $[df_{\text{pin}}/dx|_{x_{0L}}]_{T_L} = \infty$. Lowering the temperature below T_L, the function $f_{\text{pin}}(x)$ develops two branches, pinned and unpinned ones, which start and end at the boundaries $\pm x_+$ and $\pm x_-$ close to $\pm x_{0L}$. In order to decide upon the branch occupation below T_L, we have to determine the relative arrangement of the positions x_{0L} and $x_\pm$. We distinguish three cases, of which (a) is the simplest one, see Fig. 2(a), with $x_\pm$ moving away from x_{0L} in different directions. In this case, the branch occupation jumps between pinned and unpinned at $\pm x_{0L}$ and a small ac field produces a small reoccupation around these points; the relevant jumps in f_{pin} thus appear at $\pm x_{0L}$, with $\Delta f_{\text{pin}} = 2\Delta f_{\text{pin}}|_{x_{0L}}$ entering the expression for the field-cooled Campbell length [Eq. (14)]. Case (b) shown in Fig. 2(b) describes the situation where both branches grow beyond x_{0L} with decreasing temperature, $x_{0L} < x_- < x_+$. Then, vortices between x_{0L} and x_- jump to the pinned branch and
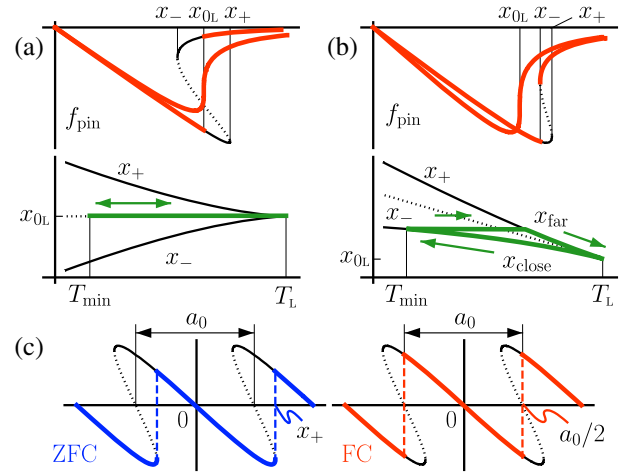

FIG. 2 (color online). Evolution of the pinning force f_{pin} crossing over from weak to strong pinning. (a) The jump in the occupation between pinned and unpinned branches first appears at x_{0L} and remains there if the branch edges at $x_\pm$ move away in opposite directions with decreasing temperature, $x_- < x_{0L} < x_+$. (b) If $x_{0L} < x_- < x_+$, the jump is pinned to x_- and hysteretic effects show up upon thermal cycling. (c) Pinscape $f_{\text{pin}}(x)$ at high magnetic fields involving only pinned and unstable branches. The relevant jumps are located at x_+ for the zero-field-cooled sample (left) and at $a_0/2$ for the field-cooled situation (right).

the relevant jump in the occupation is pinned to x_-. Accordingly, the jump in the pinning force entering λ_C is given by $2\Delta f_{\text{pin}}|_{x_-}$. Finally, case (b') involves a shrinking of the branches with respect to x_{0L}, i.e., $x_- < x_+ < x_{0L}$, and the jump in occupation is pinned to x_+, $\Delta f_{\text{pin}} = 2\Delta f_{\text{pin}}|_{x_+}$. As a result, the Campbell length λ_C may differ for the zero-field-cooled (Bean type) and field-cooled vortex states in various respects, depending on the case at hand.

Quantitative analytic results can be obtained at temperatures below but close to T_L, where $\kappa \gtrsim 1$. Expanding the bare pinning force $f_p(x)$ around x_m (where f_p'' vanishes), $f_p(x) \approx f_p(x_m) + f_p'|_{x_m}(x - x_m) - \gamma(x - x_m)^3/3$ with $2\gamma = -f_p'''|_{x_m} > 0$, we obtain the result

$$x_\pm = x_0 \pm \frac{2}{3}\sqrt{\frac{\bar{C}}{\gamma}}(\kappa - 1)^{3/2}, \qquad (15)$$

with $x_0 = x_m - f_p(x_m)/\bar{C} > x_m$ the generalization of x_{0L} to temperatures below T_L, $x_0(T_L) = x_{0L}$. The jumps at $\pm x_\pm$ then are equal and smaller than the jumps at $\pm x_{0L}$. For case (a), this results in different (by $\approx 7\%$) Campbell lengths $\lambda_C|_{FC} < \lambda_C|_{ZFC}$, while for the cases (b) and (b') the two lengths are equal. For large $\kappa \gg 1$, the three jumps are all different, resulting in different Campbell lengths with $\lambda_C|_{FC^+} < \lambda_C|_{ZFC} < \lambda_C|_{FC^-}$, where $\pm$ refer to the scenarios involving the large/small jumps at $x_\pm$.

Which of the above scenarios is realized in a specific case depends on the temperature dependence of elastic and pinning forces. Close to T_L, the behavior of $x_\pm$ is dominated by $x_0 \sim x_{0L} + a\tau_L$, with $\tau_L = 1 - T/T_L$ and the sign of the prefactor a deciding upon which case, (b) or (b'), is realized. On the other hand, for larger τ_L, the second term in Eq. (15), $\propto (\kappa - 1)^{3/2} \propto \tau_L^{3/2}$, becomes dominant and case (a) is realized.

Furthermore, hysteretic behavior of λ_C appears in cases (b) and (b') when first cooling and subsequently reheating the sample (from $T_{\min}$). Indeed, when both branches increase or decrease below x_{0L} upon cooling, the relevant jump appears at the branch edge x_{close} that is closer to x_{0L}. On reheating, the jump first remains pinned to $x_{\text{close}}(T_{\min})$ until the other edge x_{far} farther away from x_{0L} is hit, whereupon the jump follows the position $x_{\text{far}}(T)$; see Fig. 2(b). Otherwise, in case (a) or when x_{close} goes through an extremum, no hysteresis appears upon thermal cycling as long as the jump in f_{pin} is realized [21] away from the branch edges at $\pm x_\pm$.

We now briefly discuss the situation at high fields when the pinned branch extends beyond the vortex separation a_0, $x_+ > a_0/2$. Close to H_{c_2}, the bare pinning force is well approximated by the lowest harmonic, $f_p(x) \approx f_0 \sin(2\pi x/a_0)$; the competition with elastic forces then produces the multivalued function $f_{\text{pin}}(x)$ shown in Fig. 2(c). In this situation, the branch edges at $\pm x_-$ have

vanished and only the pinned branches between $\pm x_+$ survive. For the Bean state, the jump in force $(\Delta f_{\text{pin}}|_{x_+})$ determining λ_C is located at x_+. For the field-cooled state, the (slightly larger) jump in force is located at $a_0/2$ instead, hence, $\lambda_C|_{FC} \lesssim \lambda_C|_{ZFC}$; no hysteresis is expected in this regime. Upon decreasing the field, additional harmonics become relevant in the description of $f_p(x)$ and its maximal slope at x_m moves away from $a_0/2$, i.e., $x_m < a_0/2$. As x_{0L} also decreases below $a_0/2$, an unpinned branch starts developing and we cross over to the low-field domain involving both the pinned and unpinned branches. Note that neither of these regimes is small but rather occupy similar size regions within the H-T phase diagram.

In Fig. 3 we compare our main new findings, the dependence of λ_C on the vortex state and the appearance of hysteretic effects, with measurements on a single crystal superconductor SrPd$_2$Ge$_2$ (isostructural to the Fe and Ni pnictides) using a tunnel-diode oscillator technique; see Fig. 4(a) of Ref. [11] (shown are magnified traces at 0.02 and 0.3 T). A small ac excitation field $h_{\text{ac}} \approx 20$ mOe is superimposed on the dc field ensuring linearity of the response; see Ref. [22] for experimental details. Theoretical results for the Campbell lengths are found by solving Eq. (7) and extracting the relevant jumps Δf_{pin}, assuming a pinning model based on insulating inclusions [20] (we use standard Ginzburg-Landau scaling). All features, the dependence of λ_C on the state preparation, the appearance of hysteresis upon thermal cycling, as well as the reversal from $\lambda_C|_{ZFC} < \lambda_C|_{FC^-}$ at low fields to $\lambda_C|_{FC} < \lambda_C|_{ZFC}$ at high fields, are visible in the experiment and captured by the model; note that other pinning models based on metallic inclusions or δT_c, $\delta \ell$ pinning [23] (ℓ the mean free path) produce different behavior.

In conclusion, making use of strong pinning theory, we have presented a microscopic and quantitative expression for the Campbell length λ_C that captures specific properties of the pinscape. Our theory predicts the dependence of λ_C on the vortex state (FC versus ZFC) and explains the appearance of hysteretic effects, with results that are in good agreement with experiments. With the new information at hand, the pinscape can be analyzed in much more detail via deliberate
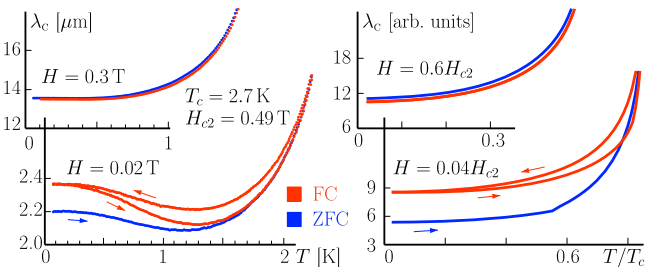
FIG. 3 (color online). Experimental (left) and theoretical (right) traces of the Campbell length $\lambda_C(T)$ for zero-field-cooled (blue curves) and (hysteretic) field-cooled (red curves) states at low (main panels) and high (inset panels) magnetic fields.

[1] A. A. Abrikosov, ZhETF **32**, 1442 (1957) [Sov. Phys. JETP **5**, 1174 (1957)].

[2] T. Halpin-Healy and Y.-C. Zhang, Phys. Rep. **254**, 215 (1995).

[3] S. Lemerle, J. Ferré, C. Chappert, V. Mathet, T. Giamarchi, and P. Le Doussal, Phys. Rev. Lett. **80**, 849 (1998).

[4] A. R. Strnad, C. F. Hempstead, and Y. B. Kim, Phys. Rev. Lett. **13**, 794 (1964); Y. B. Kim, C. F. Hempstead, and A. R. Strnad, Phys. Rev. **139**, A1163 (1965).

[5] C. P. Bean, Phys. Rev. Lett. **8**, 250 (1962).

[6] A. M. Campbell, J. Phys. C **2**, 1492 (1969); **4**, 3186 (1971).

[7] E.-H. Brandt, Z. Phys. B **80**, 167 (1990); M. W. Coffey and J. R. Clem, Phys. Rev. Lett. **67**, 386 (1991); A. E. Koshelev and V. M. Vinokur, Physica (Amsterdam) **173C**, 465 (1991); C. J. van der Beek, V. B. Geshkenbein, and V. M. Vinokur, Phys. Rev. B **48**, 3393 (1993).

[8] J. Lowell, J. Phys. F **2**, 547 (1972).

[9] A. M. Campbell, Philos. Mag. B **37**, 149 (1978).

[10] The analysis presented here does not depend on the precise dependence of $j_c(B)$.

[11] H. Kim, N. H. Sung, B. K. Cho, M. A. Tanatar, and R. Prozorov, Phys. Rev. B **87**, 094515 (2013).

[12] J. Bardeen and M. J. Stephen, Phys. Rev. **140**, A1197 (1965).

[13] R. Labusch, Crystal Lattice Defects **1**, 1 (1969).

[14] A. I. Larkin and Yu. N. Ovchinnikov, J. Low Temp. Phys. **34**, 409 (1979); A. I. Larkin and Yu. N. Ovchinnikov, in *Nonequilibrium Superconductivity*, edited by D. N. Langenberg and A. I. Larkin (Elsevier, Amsterdam, 1986), p. 493.

[15] G. Blatter, V. B. Geshkenbein, and J. A. G. Koopmann, Phys. Rev. Lett. **92**, 067009 (2004).

[16] A. E. Koshelev and A. B. Kolton, Phys. Rev. B **84**, 104528 (2011).

[17] A. U. Thomann, V. B. Geshkenbein, and G. Blatter, Phys. Rev. Lett. **108**, 217001 (2012).

[18] R. Willa, V. B. Geshkenbein, and G. Blatter, Phys. Rev. B **92**, 134501 (2015).

[19] Note that within the phenomenological approach, the Bean critical state corresponds to a vanishing curvature $\alpha = 0$; the diverging $\lambda_C \to \infty$ can be attributed to vortices penetrating deep into the sample.

[20] R. Willa, V. B. Geshkenbein, and G. Blatter (unpublished).

[21] At the minimum or maximum of $x_{\text{close}}(T)$.

[22] R. Prozorov, R. W. Giannetta, N. Kameda, T. Tamegai, J. A. Schlueter, and P. Fournier, Phys. Rev. B **67**, 184501 (2003).

[23] G. Blatter, M. V. Feigel'man, V. B. Geshkenbein, A. I. Larkin, and V. M. Vinokur, Rev. Mod. Phys. **66**, 1125 (1994).